

Assessment of Land Use Land Cover and River Dynamics of Himalaya: Seti River Sub-Basin of Nepal

Anup Raj Adhikari ¹, Sher Bahadur Gurung ^{2, *}, Laxman Adhikari ³ and Zhu Lianqi ⁴

¹ Institute of Forestry, Pokhara Campus, Tribhuvan University, Pokhara 33700, Nepal

² Central Department of Geography, Tribhuvan University, Kathmandu 44619, Nepal

³ Prithivi Narayan Multiple Campus, Tribhuvan University, Pokhara 33700, Nepal

⁴ College of Geography and Environmental Science, Henan University, Kaifeng, China

* Corresponding E-mail: sher.gurung@cdg.tu.edu.np

Article info

Keywords:

Land use land cover

Sinuosity

Water management

Change detection

Remote sensing

Received: 16th Aug. 2022

Accepted: 22nd Nov. 2022

DOI: <https://doi.org/10.3126/tgb.v9i1.55440>

© The Geographic Base

Abstract

In rapidly growing areas, land use land cover (LULC) change is one of the most pre-eminent features of environmental changes produced by human-induced activities. LULC changes are critical issues and challenges for environmentally friendly and sustainable development. Understanding land-use and land-cover (LULC) changing patterns is critical for sustainable environmental management, particularly effective water management. This study was focused on the assessment of LULC and sinuosity of the Seti River sub-Basin over 28 years. Satellite imagery of Landsat series (MS, TM, and OLI) were classified using maximum likelihood classifier to create LULC maps for 1991, 2004 and 2019. The LULC change was assessed using change detection analysis and verified the result by confuse matrix. The results showed that forest cover is regaining its original status with the increasing rate of 1.31%. In the meantime, built-up areas are expanding with the rate of 2.62% while agricultural land has decreased with the rate of -1.89% per year

and are more converted to built-up area. Trend of sinuosity index found increasing and varying in different sections of the river path indicated the complex response of changing characteristics of river flow, river mining and geomorphology of landscape. Based on research findings and descriptions from earlier works, river morphology is affected by both natural (topography, climate, precipitation), and anthropogenic (rapid urbanization, foreign labor migration, abandonment of cultivable land, community forest programs, development activities) factors.

Introduction

Land use and land cover (LULC) affects many parts of social and physical environmental aspects which has also been known as the key driving factor for ecosystem services (Rai, 2018). LULC change are the crucial indicators for environmental deviations, is the global concern of the twenty-first century. The dynamics of LULC are of immediate concern from several perspectives and across various spatial and temporal scales, including climate change, biodiversity loss, land management and ecosystems services (Bagan., 2014; Ellis., 2006). LULC change is a dynamic process that occurs on biophysical surfaces throughout time, and space is important in natural resource studies. The assessment of global environmental changes and natural resource management increasingly view

LULC alterations as a major and critical component. (Kumari, 2019; Lambin, 1997; Rawat., 2013). Anthropogenic and natural variables are the primary drivers of LUCC. It is widely accepted that anthropogenic activities have had a considerable impact on global spatial patterns of land use (Deng et al., 2009). Similarly, local climate and weather, elevation, bedrock and soil type, surface water, and groundwater are important biophysical components at the land unit level (Verheye, 2009).

One of the most obvious effects of anthropogenic activity at the local, regional, and global levels is its effects on LULC. Land use alteration has wide ranging environmental impacts influencing ecological balance and ecosystem services such as nutrient cycling, climate regulation and water treatment (Hu, 2008). Majority of the studies revealed that LULC alteration negatively influenced the environmental resources and ecological functions. Agriculture's needs prompted deforestation, which reduced forest areas and accelerated soil erosional processes (Uddin, 2010). Unprecedented population growth, which has turned into significant issue in many cities, is one of the causes of the LULC change. The Land Use and Land Cover (LULC) change can alter groundwater dynamics, hydrological cycles (Kayet., 2019; Sun et al., 2011) and degrade aquatic

environment resulting severe impact in the environmental characteristics of the watershed (Rimal et al., 2015). Land use patterns have the potential to raise a number of risks, including sewage mixing owing to fast urbanization, non-point sources of pollution, and sedimentation from soil erosion in upstream regions (Adhikari et al., 2018).

LULC pattern is determined by complex interaction of bio-physical and socioeconomic scenario of the area. Analyzing LULC change pattern and understanding their driving factors is important for sustainable land use planning (Rai et al., 2018). Change detection represents monitoring of the vegetation through time and determine what sort of variation in succession are taking place. Measurement of LULC change of various land characteristics across various time periods is the primary goal of the change detection procedure based on digital photographs (Reis, 2008). Satellite images are used to routinely monitor change in order to develop future urban land regulations and plans that will be appropriate (Rai et al., 2020).

River channel shift affects the LULC of the surrounding basin area (Debnath et al., 2017). River maintains its equilibrium condition by erosion and deposition process. Changes in river channel can alter aquatic and riparian ecosystem, and bring flood hazard and

difficulties in navigation management (Deb & Ferreira, 2015). Monsoon flood is a frequent hazard in the Tarai Region of Nepal. Changes in precipitation patterns and human interventions were identified as the main causes of flood hazard and indicated change in river morphology (Crosato et al., 2012; Karki et al., 2011; Thakur & Singh, 2018). Human activities such as deforestation, extension of agriculture land into river floodplains, gravel extraction from river bed is taking place within the catchment areas. River margins have been interrupted by such human activities which led to change in river morphology (Yousefi et al., 2016). Flood, river sedimentation and river bank cutting have resulted agriculture land and residential area loss; showing avulsion tendencies and variations in meandering of river (Karki et al., 2011).

LULC change has severe impact on watershed's hydrological regime such as change in total runoff, alteration of peak flow characteristics, decline in water quality and changes in river's amenities (Ruslan, 2003). In other word change in LULC pattern has direct implication on river hydrology (Garg et al., 2019) by triggering water induced disaster like landslide, floods and drought. The studies of river dynamics are thus fundamental for the management and planning of the river behavior. It is essential for the development of environmentally

acceptable and sustainable river-based projects.

Lack of adequate research and historical data on LULC changes hindering implementation of efficient mitigation measures. Moreover, most of LULC research has been limited to national level with little in regional scale (Paudel et al., 2016). The shift in LULC pattern is the outcome of project activities such as road construction, heavy vehicles movement thereby increases vulnerability of mountain landscapes and biodiversity of flora and fauna. Change in LULC pattern has direct implication on river hydrology (Garg et al., 2019) which particularly triggered water induced disaster like landslide, floods, and drought. Majority of the initial project activity such as gravel extraction alongside the riverbed which may have followed up for the change in river dynamism resulting in both temporary and permanent channel instability (Wishart et al., 2008).

Geospatial Information Systems and remote sensing are frequently utilized to provide precise and timely data on the spatial distribution of land use/land cover changes over vast areas (Dezso et al., 2005; Guerschman et al., 2003; Rogan et al., 2004). For the detection of LULC patterns, RS and GIS have been particularly effective (Chaudhry et al., 2015; Chen, 2018; Nuez et al., 2008; Rahman et al., 2012). A reliable and

affordable technique for tracking LULC changes has been demonstrated by the combined use of satellite RS and GIS (Hazarika et al., 2015; López-Granados et al., 2013; Serra et al., 2008).

The aim of this research is to assess LULC status, trend and river sinuosity in the Seti basin. This research outcome is important for policy makers, public officials, and various stakeholders to include multiple hazard risk mitigation in land use policies and plans. Monitoring of LULC in watershed area and its impact on river hydrology is helpful to design environment friendly development planning and preparing future strategy for disaster management. Thus, establishing connections between urban expansions, escalating population growth, haphazard mining of construction materials and multiple hazards and risk assessment will also improve in modelling the latent impact of future catastrophes and emergency preparedness.

Methods and Materials

Study area

The entire Seti River basin incorporates of five districts: Kaski, Tanahu, Parbat, Syangja and Lamjung. It covers a total area of about 2922.63 square km. The study area is a sub-watershed of Seti River extending from latitude 28°19'35" to 28°04'32" N and longitude 83°57'33" to 84°04'07" E draining up the total

area of 682.08 km² (68207.94 hectares). Administratively, the study area covers Annapurna, Machhapuchhre, Madi and Rupa rural municipalities and Pokhara Metropolitan city of Kaski district, Shuklagandaki Municipality of Tanahu district. The study area also extends over the small portion of Aadhikhola and Phedikholra rural municipalities of Syangja district and Kushma municipality and Modi rural municipality of Parbat district. 97.26% of the study area lies in Kaski district whereas 2.38%, 0.22% and 0.14% of the area lies in Tanahu, Syangja and Parbat districts, respectively. The study region is between 499 and 5476 meters above mean sea level. The main Seti tributaries within the defined sub-basin are Mardi Khola, Kali khola, Phedi khola, Bijayapur khola, and Khudi khola. The area's main water sources include Phewa Lake, Begnas Lake, Rupa Lake, Dipang Lake, Khaste Lake, Maldi Lake, Gunde Lake, and Niureni Lake.

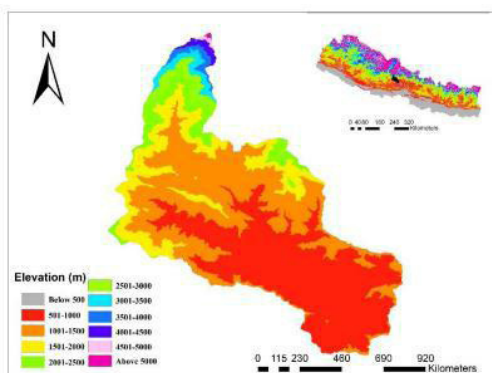


Figure 1. Study Area

Data sources

Field data

Field data were collected in October 2019 to analyze the status of land use and land cover status over the study area. A total of 180 random locations were selected for the collection of the field data and about 350 Global navigation satellite system (GNSS) points covering most of the LULC classes were obtained during fieldwork in the months of November and December 2019.

Satellite images

The classification process and analysis of the different LULC classes were done using Landsat satellite image covering the Landsat 4-5 TM acquired on 12 October 1991, Landsat satellite image covering the Landsat 7 ETM+ acquired on 26 February 2004, as well as a Landsat satellite image covering the Landsat 8 OLI/TIRS acquired on 10 November 2019 (Table 1). The USGS Earth Explorer platform allowed for the download of satellite pictures with a spatial resolution of 30m by 30m (www.earthexplorer.com). Images from the winter months were chosen as the primary sources of data for this study (Uddin et al., 2010).

Similarly, DEM covering the Shuttle Radar Topography Mission (SRTM) 1 Arc-Second Global acquired on 23 September 2014 was downloaded from USGS Earth Explorer.

Table 1. Details of remotely sensed satellite images used in this study

Year	Landsat Sensor	Acquisition date	Path/Row	Resolution	Bands used
1991	4-5 TM C1	October 12,1991	142/40	30m	1,2,3,4,5,6 and 7
2004	7 ETM+ C1	February 26,2004	142/40	30m	1,2,3,4,5,6,7 and 8
2019	OLI/TIRS C1	November 10, 2019	142/40	30m	1,2,3,4,5,6,7,8, 9,10 and 11

Image processing and classification

Preprocessing is the primary step for image classification which helps in adjusting the blur and distortion in the original images finally providing the nearest results to the real image (Yang et al., 2019). The preprocessing steps such as band stacking, radiometric correction and atmospheric correction were carried out by using ENVI 5.3. Landsat 7 ETM+ inputs are not gap-filled in Surface Reflectance production, and gapped areas are not processed for Surface Reflectance. Therefore, scanline error of 2004 satellite image was removed, and correction were carried out to convert the DN to surface reflectance.

Each image in the LULC database was processed using the commonly used supervised classification method utilizing the Maximum Likelihood classifier algorithm (Bailly et al., 2007; Liu et al., 2002; Manandhar et al., 2009; Mandal & Mandal, 2014; Zubair & Ji, 2015). The false color composite was used to create random samples from the composition of several bands as training points/regions of interest (ROI). For the

supervised classification strategy, the ROIs were chosen as the signatures for each land class. For the classification of the photograph, six separate terrain classifications were created (Table 2).

Table 2. Description of LULC classes

Land Use Types	Description
Forest	Evergreen, Sparse Forest area, Private Forest, Grassland with scattered trees
Agricultural Land	Cultivation land, Ploughed land, Seasonal land, Terrace land
Built-up Area	Settlement areas, Human infrastructures, Construction sites
Barren Land	River banks, Bare ground, Landslide zones
Water Bodies	Rivers, streams, lakes, ponds, swamps and wetlands
Snow Cover	Snowcapped area

Enough training pixels for each spectral class were obtained to allow reasonable estimates. The set of random training samples were increased to improve parameter estimates. On average, about 350 training samples were collected

from each of the land classes. Known representative pixel for each class was chosen and a training data was formed. Areas of the classes are measured by producing class maps and tables which summarize class membership of all pixels in an image. Pixel based vectors are grouped into spectral classes using training samples and ground cover types of interest and are represented via mapping.

Accuracy assessment

In order to determine how accurately the classification depicts the real world, accuracy assessment involves comparing a classified satellite image with ground-truth data. By the creation of a classification error matrix, accuracy assessment objectively evaluates the effectiveness of pixels sampled into the appropriate land cover classes (Rwanga, 2017); (Lillesand et al., 2015). Free high-resolution satellite pictures from Google Earth are crucial resources for confirming the LULC categorization (Tilahun & Teferie, 2015). In this study, a Google Earth image is used to validate the accuracy rating. More than 300 points in all were made and distributed at random within the research area's categorized image. Each reference point's best guess was used to fill the accuracy evaluation cell array reference column. High-resolution Google Earth images from the year 2004 were used to gather ground truth data for these sites. Less samples from the tiny areas of land cover types, including snow cover and water bodies, were chosen to

validate the classified data than from the larger areas, like agricultural land and forests. To verify the accuracy of the 1991 land cover database, topographical maps were used as references. Through the use of a confusion matrix table, the relationship between points in the Landsat categorized data and related reference points was discovered. Matrix was created in MS Excel and accuracy assessment was carried based on the calculation of the overall accuracy, user's accuracy, producer's accuracy, and kappa coefficient.

Change detection of LULC classes

To examine the pattern and trend of change in the research area, change detection analysis was done on Landsat photos from three separate years. LULC maps were created for the years 1991, 2004 and 2019 from Landsat satellite imagery using GIS.

The land use type of 1991, 2004 and 2019 has been categorized into forest, agricultural land, built-up area, barren land, water bodies and snow cover. Area and change statistics were calculated and analyzed for these six classes. The area for each class was calculated using the field calculator in the attribute table of the supervised layer. The

area for each class was calculated for the years 1991, 2004 and 2019. The change in area for each class was calculated for intervals 1991-2004, 2004-2019 and 1991-2019. Change detection comparison (pixel by pixel) technique was applied to

the Land use Land cover maps derived from satellite imagery (Reis, 2008). Map representation of change between each Land use classes were prepared using conversion tools before following different Geoprocessing techniques through ArcGIS. By using the change detection statistical tool of the post classification, the matrix table of “from – to” change class was obtained. Similarly, the increasing and decreasing percentage were extracted from the area of each map from each classified image.

The annual rate of change per class were calculated to determine the pattern of land use change in the sub-Basin by using the equation (Reis, 2008).

$$P = (100/t2 - t1) \times \ln A2/A1$$

where, A1 and A2 are the land cover of a particular class at time t1 and t2, respectively and P is the percentage of change per year.

Change in river dynamics

River dynamics usually represents the channel morphology which describes the shapes of river channels and how they change in shape and direction over time. Deposition or erosion potential, deviation of meander geometry etc. are some variables that measure dynamism of a river (Tamrakar et al., 2011). Thus, to understand the dynamism in river, sinuosity of the Seti River over the past three decades was calculated.

The Landsat satellite images with the different multispectral band combinations were used to extract bank lines from the images and a river polygon shapefile was created in ArcMap. The time series of data covered the period from October 1991 to November 2019. Centerlines were created from the river shapefile polygon. The channel length and air measurements were taken from the centerlines of different years respectively. Equal spacing of 5 km divides the entire river into 9 strips from Ghachowk to Kotre in the delineated Seti Basin. The sinuosity was analyzed in these very 9 sections.

Channel Index or total sinuosity index is the ratio of the length of the river channel under study to the shortest air distance between the source and mouth of the channel (Friend & Sinha, 1993; Mueller, 1968). Sinuosity Index = CL/Air

CL= the length of the river channel under study

Air = the shortest air distance between the source and mouth of the river channel

Rivers with sinuosity index less than 1.05 are referred to as straight, between 1.05 and 1.3 are referred to as sinuous, and between 1.3 to 1.5 regarded as moderate meandering and above 1.5 are cited to be as in meandering form (Horacio, 2014) (Figure 2).

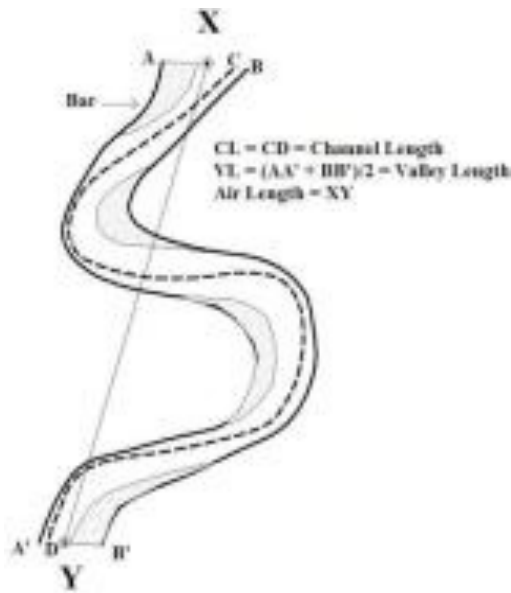


Figure 2. Parameters taken for Mueller's sinuosity index (Ghosh & Mistri, 2012)

Results and Discussion

Land use land cover pattern over the study area

LULC classification of 1991 showed that Agricultural land was the major

Land use class covering 51.9% of the area followed by Forest, Barren land, Built-up area, Water bodies and Snow cover covering 37.85%, 4.62%, 3.63%, 1.71% and 0.29% area respectively. The result of 2004 showed that Forest has overtaken Agricultural land as the major Land use class covering 48.36% of total area. Agricultural land's coverage decreased to 39.96% of the total sub-basin which is then followed by Built-up area (5.81%), Barren land (3.52%), Water bodies (1.80%) and Snow cover (0.55%). Similarly, the LULC map of 2019 showed that Forest area was still the major Land use class occupying 54.64% of the total area of the sub-basin. Agricultural land, Built-up area, Barren land, Water bodies and snow cover covered 30.38%, 7.49%, 5.98%, 1.36% and 0.15% of the area respectively (Figure 3).

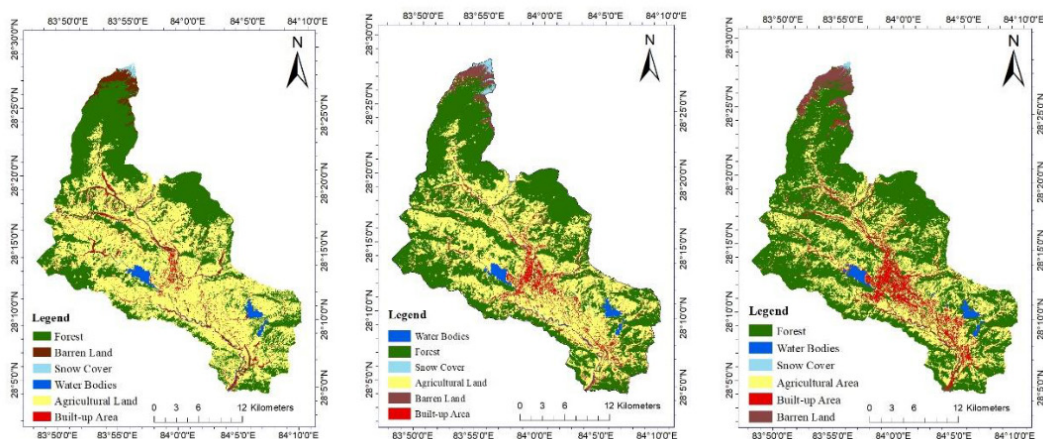


Figure 3. Land use and land cover maps for 1991, 2004 and 2019 (left to right)

LULC classification accuracy

The classification accuracy was computed within the range of 72% to 100% by user's and 61% to 100% by producer's accuracy in 2019. Similarly, in 2004, the user's and producer's accuracy were computed within the range of 77% to 93% and 52% to 100%, respectively. The range of user's and producer's accuracy was found to be within 76% to 94% and 58% to 94% respectively in 1991. The overall accuracy was calculated by 81.52%, 85.25% and 88.25% in 1991, 2004 and 2019, respectively. The Kappa statistics are almost perfect rank (0.81–1.00) that computed by 0.803 and 0.843 for 2004 and 2019, respectively. In 1991, the Kappa coefficient of 0.754 was obtained which is rated as substantial.

LULC dynamics over the period 1991 to 2004

The result showed that forest area followed by the area covered by built-up area, water bodies and snow cover has increased while agricultural area and barren area has decreased during this period (Figure 4). The highest change has seen in agricultural land decreased by 8148.87 hectares followed by increment of forest area by 7164.67 hectares. Forest area had occupied 37.85% of the total area of the sub-basin which increased

at the rate of 1.90% ending up covering 48.36% of the area till 2004. The change rate is then followed by built-up area with the rate 3.69% adding up 114.76 hectares per year over 13 years. Agricultural land and barren land have decreased with the rate of -1.99% and -2.06% respectively within this period (Table 3).

The change matrix helps to observe the land that has been transferred into new class within different time phase. The horizontal rows represent total area of 1991 while the vertical column represents the total area of 2004. The table illustrates that 1.82% of forest from 1991 was converted into agricultural land in 2004. The highest change was seen in agricultural land covering 12.39% of area being converted into forest. The 2.04% of cultivable area was converted to settlement area during this period. At the same time 1.08% barren land was converted to agricultural land.

The climate-sensitive snow cover decreased by about 52 percent from 1991 to 2004. Most of the snow cover turned into barren land. Similarly, barren land decreased by about 23 percent during the period and most of the barren land was used for agricultural activities.

Table 3. LULC change matrix (1991-2004)

Class	2004						
	Forest	Agricultural Land	Built-up Area	Barren Land	Water Bodies	Snow Cover	Total
Forest	35.198	1.823	0.132	0.524	0.027	0.146	37.850
Agricultural Land	12.396	36.651	2.043	0.622	0.194	0.002	51.908
Built-up Area	0.026	0.234	3.062	0.289	0.011	-	3.622
Barren Land	0.697	1.086	0.518	1.935	0.253	0.131	4.621
Water Bodies	0.035	0.166	0.055	0.125	1.315	0.010	1.705
Snow Cover	0.02	-	-	0.028	-	0.257	0.287
1991 Total	48.354	39.967	5.811	3.521	1.799	0.546	100

LULC dynamics over the period 2004 to 2019

Forest area, built-up area and barren land gained the area with the rate of 0.82%, 1.70% and 3.59% respectively. There was decrease in area of agricultural land and snow cover with the rate of -1.81% and -8.49% respectively. The area covered by water bodies also shrank with the rate of -1.84% in this time though its area had increased during 1991-2004 (Figure 4).

Change matrix was computed for the period which gave the transition between

all classes from 2001 to 2011 which is presented in the table below. The change matrix thus obtained illustrates that 1.3%, 0.27% and 0.89% of forest area had been transformed to agricultural land, built-up area, and barren land, respectively. The maximum amount of transition was seen in agricultural land, 8.21% of agricultural land being changed into forest area. 1.33% of agricultural land, 0.32% of barren land and 0.004% of water bodies from 2004 were transformed into built-up area in 2019 (Table 4)

Table 4. LULC change matrix (2004-2019)

Class	2019						
	Forest	Agricultural Land	Built-up Area	Barren Land	Water Bodies	Snow Cover	Total
Forest	45.799	1.380	0.266	0.894	0.008	0.007	48.354
Agricultural Land	8.206	28.307	1.325	2.084	0.039	-	39.967
Built-up Area	0.072	0.095	5.548	0.092	0.004	-	5.811
Barren Land	0.311	0.508	0.315	2.370	0.014	0.003	3.521
Water Bodies	0.055	0.090	0.033	0.245	1.298	0.078	1.799
Snow Cover	0.191	-	-	0.298	0.001	0.056	0.546
2004 Total	54.634	30.38	7.487	5.983	1.362	0.145	100

LULC Dynamics over the period 1991 to 2019

Over the time of 28 years; forest, built-up area and barren land has increased whereas agricultural land, water bodies and snow cover has decreased in the Seti sub-basin (Figure 4). There is a difference of 16.79% of total area covered by forest which has increased at the rate of 1.31% over these three decades. Agricultural land holding of about 51.9% of the total area has decreased with the rate of -1.89% ending up covering 30.38% of the area. The overall change rate per class yearly is maximum for built-up area that is 2.62% per year. Barren land has gained its area with the rate of 0.93%. The land cover classes with decreasing rates along with agricultural land are water bodies

and snow cover with the rate of -0.79% and -2.4% respectively.

The overall change matrix explains that large amount of agricultural land has been converted to forest area. 18.70% of agricultural land in 1991 was transformed into forest area in 2019. Similarly, 3.83%, 1.65% and 0.04% of agricultural land was converted into built-up area, barren land, and water bodies, respectively (Table 5). During these three decades, agricultural land to forest, agricultural land to built-up area, agricultural land to barren land, forest to agricultural land, forest to barren land, barren land to forest, water bodies to barren land, water bodies to agricultural land and snow cover to barren land were some of the recognizable transformations.

Table 5. LULC change matrix (1991-2019)

Class	2019						
	Forest	Agricultural Land	Built-up Area	Barren Land	Water Bodies	Snow Cover	Total
Forest	34.771	1.379	0.179	1.518	0.002	0.001	37.850
Agricultural Land	18.708	27.683	3.827	1.650	0.040	-	51.908
Built-up Area	0.079	0.231	3.007	0.289	0.016	-	3.622
Barren Land	0.978	0.982	0.318	2.267	0.069	0.007	4.621
Water Bodies	0.064	0.106	0.156	0.144	1.234	0.001	1.705
Snow Cover	0.035	-	-	0.115	0.001	0.136	0.287
Total	54.635	30.381	7.487	5.983	1.362	0.145	100

1991

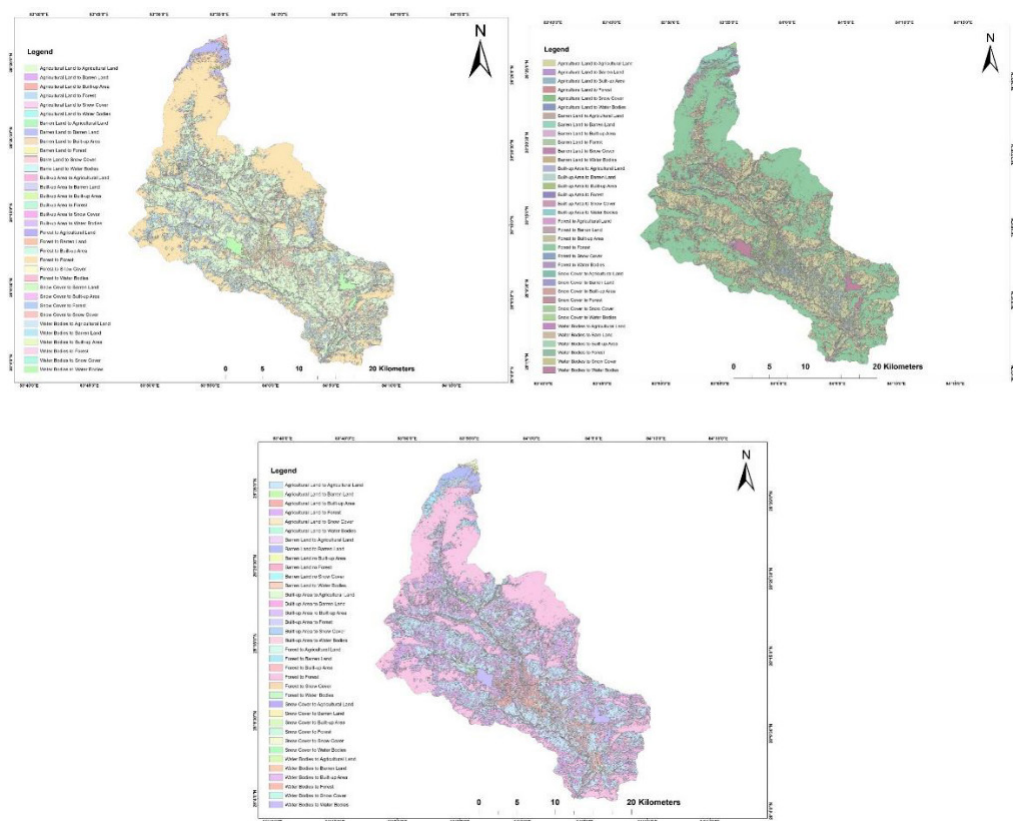


Figure 4. LULC Change map for the year 1991-2004, 2004-2019 and 1991-2019(left top to bottom right)

Change in river dynamics

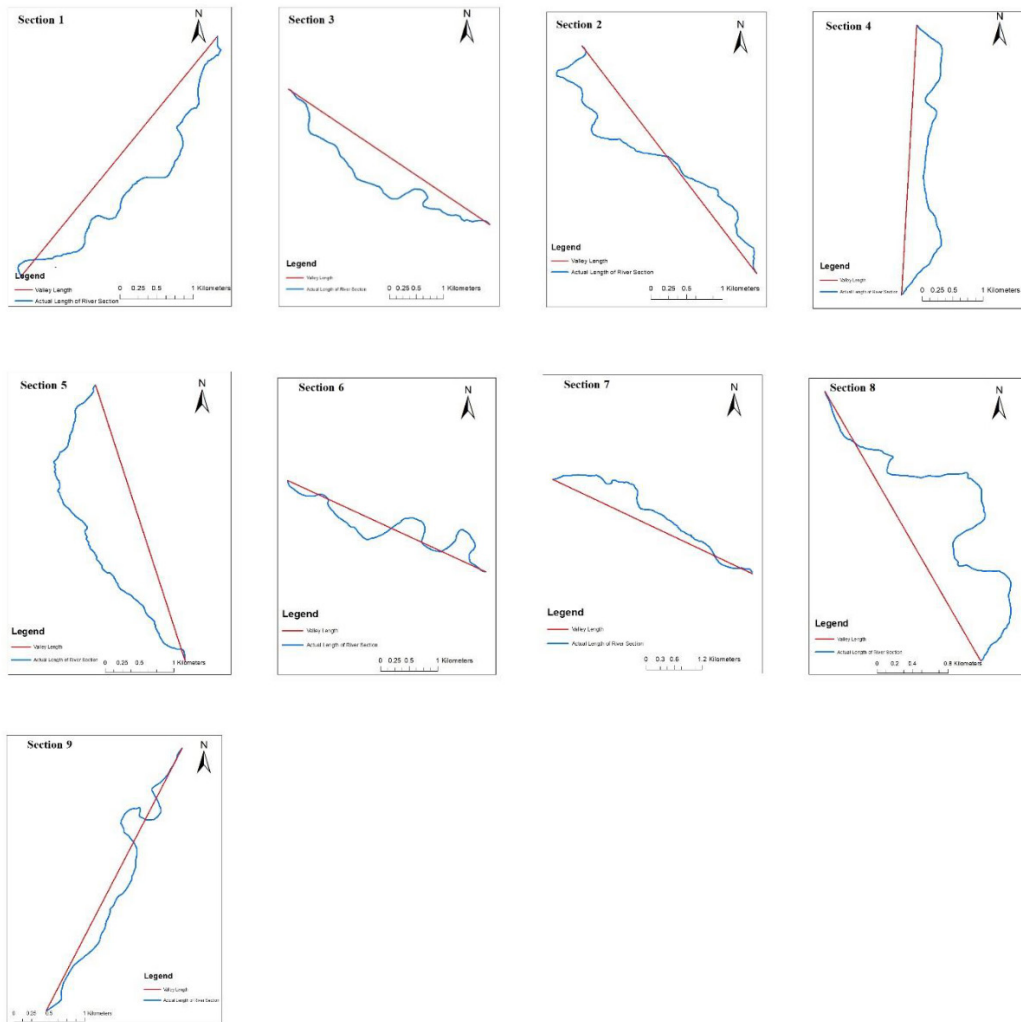


Figure 5. Sections of Seti River

The sinuosity index value ranges from 1.11 to 1.52 in 1991, 1.10 to 1.42 in 2004 and 1.13 to 1.47 in 2019. The average sinuosity index was found to be 1.25, 1.24 and 1.25 in the years 1991, 2004 and 2019, respectively (Table 6). The river was found to be in the category of sinuous

(1.05-1.3) over the past three decades. A straight stream has sinuosity 1.0 and as this number increases the stream departs from a straight line (Schumm, 1963).

Table 6. Sinuosity index at different intervals of time

Section	Sinuosity Index at 1991	Sinuosity Index at 2004	Sinuosity Index at 2019
1	1.184161	1.214461	1.223256
2	1.247572	1.27772	1.28656
3	1.24633	1.227397	1.204096
4	1.107696	1.103318	1.12901
5	1.163801	1.150186	1.196313
6	1.479327	1.42426	1.44631
7	1.214303	1.204131	1.166161
8	1.523418	1.405674	1.467548
9	1.202352	1.212974	1.216407
Average	1.250339	1.238818	1.250118

In 1991, most of the sections were found to be in sinuous form while the sixth section was found to be moderately meandering and the eighth section was found to be meandering category with the sinuosity value of 1.52. Between 1991 and 2008, the value of sinuosity index increased in the first, second and ninth sections whereas the value had decreased in rest of the six sections. The greatest increase of value was seen in Section 1 (0.0303) and the eighth section experienced greatest decrease in SI value (-0.11774) in between this period.

Similarly, in both years 2004 and 2019, except the sixth and ninth sections which were moderately meandering all the other

sections were found to be sinuous. In between these two periods (2004-2019), the value of sinuosity index increased in first, second, fourth, fifth, sixth, eighth and ninth sections while the other sections third and seventh experienced the fall in value of sinuosity index. Eighth section experienced the greatest increase (0.061874) in SI value whereas the greatest decrease was seen in seventh section (- 0.03797) in between the years 2004 and 2019.

Spatio-temporal dynamics of LULC

Human actions are responsible for the alteration of the terrestrial environment at unprecedented rates, magnitudes, and

spatial scales. Human induced landcover change is a major element of global environmental change. The Seti sub-basin can be considered as an important east–west stage point in the trans-Himalayan trade route since the medieval age (Poudel, 2008), center of religious gatherings and a permanent marketplace experiencing speedy urbanization and population growth. In the last three decades, there has been great transition in the dynamics of the land use pattern over the Seti sub-basin. The area has gained about 16.8% of the forest and lost 21.52% of cultivable land, attaining about 3.86 % of the urban area within the same time.

The study area experienced the great increase in forest area over these past three decades. The increase in forest has been aided by the better management of the forest through introduction of community forest programs, forest act and forest regulation in middle mountains (Bhandari & Grant, 2007; Lamichhane, 2008; Neupane, 2016; Niraula et al., 2013), reduction in the dependency of the fuelwood (Chaudhary & Rimal, 2017; Pandey et al., 2016), decreasing dependency on forest for manure and grass (Balla et al., 2014), relinquishment of cultivable land etc. The positive changes in forest cover provide some evidence of ecological sustainability of the resource. These findings also signify the success of forest conservation efforts by local communities and external agencies involved to some extent. The general improvement in forest cover

after the implementation of community forestry program indicates the relative superiority of community-based forest governance over government control of the resource.

Agricultural land coverage showed a decrease of 11.94% and 9.58% between 1991-2004 and 2004-2019 respectively. Equivalent results were observed by (Rimal et al., 2015) in the Pokhara valley where agricultural land decreased by 2.5% between 1990 and 2013. Likewise (Rimal, 2013) revealed that agricultural land decreased by 60.73%, 52.76%, 38.70% and 20.27% in 1977, 1990, 1999 and 2010, respectively, within Pokhara sub-metropolitan city. Most of the studies conducted on middle mountains of Nepal showed increasing migration trend of youth to towns and cities due to lack of employment opportunities and political stability which led abandonment of cultivation land (K. C. et al., 2017). In the middle mountains of Nepal 33% of the agricultural land has been abandoned (Paudel et al., 2012). The increasing trend of urbanization and abandonment of agricultural land might be the major influencing factors in decrease of cultivable land across Seti sub-basin.

Land coverage of the built-up area has the highest rate of change among the six different classes over the study area. There are several studies that resembles the result of our study. Urban/built-up area in Kaski district, which occupies major portion of the sub-basin which totaled 24.06 km² in 1988, increased

to 60.74 km² in 2016 experienced the largest transformation during this period (Rimal et al., 2018). Population growth, changing urban definitions and expansion of municipal boundaries are the primary elements responsible for the rapid increase in settlement areas (Rai et al., 2020). Economic opportunities, population growth and migration, public service accessibility, globalization, the physical condition, tourism, plans and policies, the land market and political factors

are the major drivers resulting in rapid urbanization in the Seti sub-basin (Rimal, 2011; Rimal et al., 2015). Urbanization is based mainly in the social development with the specification and characteristics in the specific subject matters such as physical infrastructure development, economic and commercial development which directly contribute to the loss of cultivated land. Although urban areas cover a small fraction of the world's land surface, their rapid expansion has significantly altered the natural landscape and created enormous environmental, ecosystem, and social impacts (Berling-Wolff & Wu, 2004; Mundia & Murayama, 2010; Weber et al., 2003). Regular monitoring of the growth is thus necessary to control haphazard growth, reduce potential environmental and socioeconomic risks, and formulate appropriate urban land policies and plans in the future. Barren land though showed a decrease from 1991-2004, its area has increased over the time period of last

three decades. Seti sub-basin consists of the area which receives the highest precipitation in a year which leaves the sub-basin exposed towards the multiple hazards such as avalanches, debris flow, landslides, soil erosion, sinkholes, land subsidence etc finally increasing the barren area (Jaquet et al., 2015; Khanal & Wantanbe, 2006). Barren land increased in Kaski district increased mainly because of the significant decrease of snow cover (Rimal et al., 2018). Increasing abandonment of agricultural land has raised vulnerability towards various geomorphic changes leading towards the formation of bare land (Khanal & Wantanbe, 2006).

The water bodies in the sub-Basin are primarily comprised of eight different lakes of Pokhara Metropolis. The area of water bodies has reduced with the rate of 0.79% over the period of 28 years decades. The lakes have been shrinking through several reasons such as sedimentation, encroachment, haphazard construction of road and direct disposal of pollutants. Rural road constructions and other developmental activities cause more soil erosion which facilitates the transport of sand and gravel into the lake (Adhikari et al., 2018). There is need of proper land use policy for the control of increasing sedimentation and vulnerability towards various hazards responsible for degradation of water bodies. The LULC management prescriptions for the Lake watershed present in the sub-Basin can include construction of small

water and soil conservation structures, such as check dams, percolation ponds, etc.; participation of rural people and stakeholders to prevent further land degradation, and to reduce soil erosion; and improvement in agriculture production following better agricultural practices (Regmi et al., 2017).

The result revealed that the snow cover is being decreased across the study area. The snow cover has been decreasing trend in Nepal Himalayas; the glacier cover decreased by 24% over the country between 1977 and 2010 (Bajracharya et al., 2014). The status of change in snow/glacier area reported by most research is a high rate of shrinkage from past times to recent decades, and it is predicted that this will continue at a rapid rate in the future

Sinuosity of Seti River

Sinuosity has differed in different sections over the different time period. Sinuosity is topologically controlled as the river adjusts its initial courses to the irregularities of the surface. Additional sinuosity is imminent when the river has down cut sufficiently to allow the formation of floodplain; properties inherent in flowing water tend to promote lateral migration of the channel upon the floodplain (Mueller, 1968). River supplied with large load of pebbles, gravels, sand, which are transported as bed load; increase sinuosity due to erosional and depositional processes resulting in migration of channel (Sapkale et al.,

2016). Seti has created stupendous gorges ranging the depth between 50 meters to 80 meters for about 5.6 km of the subbasin. This might be a reason for the constant sinuosity over the three decades among some of the sections. Factors including sand and gravel extraction and riverbed regulation decrease flow rate and riverbed slope which affects river plan form which finally decreases the sinuosity of the river (Ozturk & Sesli, 2015). Thus, fluctuating sinuosity index value in the sixth and eight sections might be the result of presence of the extraction companies on the very sections which was confirmed through Google Earth.

Conclusion

This study provides several insights on potential factors affecting LULC and shift river morphology in the Seti watershed of Nepal. This study provides a knowledge base for policy makers to plan sustainable and efficient watershed management.

The obtained land use land cover maps summarized the highest coverage in the area by forest and agriculture followed by other four classes in all three dates. The result shows that the forest area and built-up area has increased remarkably by 16.79% and 3.86% respectively compared to other LULC classes over the same time periods (1991 to 2019). This can be attributed to various driving factors. The rate of built-up expansion in this period is maximum with an annual increasing rate of 2.63%. Agricultural land has marked the greatest decrease of

21.52% area with a rate of -1.89% per year in the period 1991 to 2019. Agriculture is major class contributing to the built-up expansion in the area. The area covered by water bodies in the sub-basin has been decreasing with the rate of -0.79% over this time period. Bare area has slightly increased 0.93% per year and snow cover was found to be decreasing with the rate - 2.41% in the Seti sub-basin over the last three decades. Change matrix revealed that the agricultural land being converted to forest and built-up area were the major transformations over the three decades.

The morphometric parameter: sinuosity of the Seti River was observed during the period of 1991-2019. The study was analyzed by dividing the river into 9 sections. The sinuosity index of Seti River ranges from 1.10 to 1.52 in the period 1991-2019. Sinuosity exhibited distinct characteristics in different sections. The overall average sinuosity was calculated as 1.24 which represents that the channel is sinuous.

References

- Adhikari, N., Pant, R. R., Rimal, B., & Rai, R. (2018). Land Use and Land Cover Change in Western Nepal: A Case from Phewa Watershed-Pokhara, Nepal. *Himalayan Scientific Journal*, 9, 33-42. <https://www.researchgate.net/publication/329521319>
- Bagan, H., & Yamagata, Y. (2014). Land-cover change analysis in 50 global cities by using a combination of Landsat data and analysis of grid cells. *Environmental Research Letters*, 9(6), 064015. <https://doi.org/10.1088/1748-9326/9/6/064015>
- Bailly, J.S., Arnaud, M., & Puech, C. (2007). Boosting: A classification method for remote sensing. *International Journal of Remote Sensing*, 28(7), 1687–1710. <https://doi.org/10.1080/01431160500469985>
- Bajracharya, S. R., Maharjan, S. B., & Shrestha, F. (2014). The status and decadal change of glaciers in Bhutan from the 1980s to 2010 based on satellite data. *Annals of Glaciology*, 55(66), 159-166.
- Balla, M. K., Tiwari, K. R., Kafle, G., Gautam, S., Thapa, S., & Basnet, B. (2014). Farmers dependency on forests for nutrients transfer to farmlands in mid-hills and high mountain regions in Nepal (case studies in Hemja, Kaski, Lete and Kunjo, Mustang district). *International Journal of Biodiversity and Conservation*, 6(3), 222-229. <https://doi.org/10.5897/IJBC2013.0670>
- Berling-Wolff, S., & Wu, J. (2004). Modeling urban landscape dynamics: A case study in Phoenix, USA. *Urban Ecosystems*, 7(3), 215–240. <https://doi.org/10.1023/b:ueco.0000044037.23965.45>

- Bhandari, B., & Grant, M. R. (2007). Land use and population dynamics in the Kalikhola watershed of Nepal. *Journal of Rural and Community Development*, 2(2).www.jrcd.ca
- Chaudhry, S., Attri, P., & Sharma, S. (2015). Remote Sensing & GIS based Approaches for LULC Change Detection-A Review. *International Journal of Current Engineering and Technology* 5(5), 1 – 12, INPRESSCO. <http://inpressco.com/category/ijcet>
- Chen, Y. (2018). Improved relative radiometric normalization method of remote sensing images for change detection. *Journal of Applied Remote Sensing*, 12(04), 1. <https://doi.org/10.1117/1.jrs.12.045018>
- Deb, M., & Ferreira, C. (2014). Planform channel dynamics and bank migration hazard assessment of a highly sinuous river in the north-eastern zone of Bangladesh. *Environ Earth Sci* 73 (10): 6613–6623.<https://doi.org/10.1007/s12665-014-3884-3>
- Debnath, J., Das (Pan), N., Ahmed, I., & Bhowmik, M. (2017). Channel migration and its impact on land use/land cover using RS and GIS: A study on Khowai River of Tripura, North-East India. *Egyptian Journal of Remote Sensing and Space Science*, 20(2), 197–210. <https://doi.org/10.1016/j.ejrs.2017.01.009>
- Deng, J. S., Wang, K., Hong, Y., & Qi, J. G. (2009). Spatio-temporal dynamics and evolution of land use change and landscape pattern in response to rapid urbanization. *Landscape and urban planning*, 92(3-4), 187-198.<https://doi.org/10.1016/j.landurbplan.2009.05.001>
- Devkota, L., Crosato, A., & Giri, S. (2012). Effect of the barrage and embankments on flooding and channel avulsion case study Koshi River, Nepal. *Rural Infrastructure* 3 (3), 124-132.(2012). <https://www.researchgate.net/publication/265420413>
- Dezso, Z., Bartholy, J., Pongracz, R., & Barcza, Z. (2005). Analysis of land-use/land-cover change in the Carpathian region based on remote sensing techniques. *Physics and Chemistry of the Earth, Parts A/B/C*, 30(1-3), 109-115. <https://doi.org/10.1016/j.pce.2004.08.017>
- Ellis, E., & Pontius Jr, R. G. (2006). Land-use and land-cover change—encyclopedia of earth. *Environ. Protect*, 2, 142-153.
- Friend, P., & Sinha, R. (1993). Braiding and meandering parameters: Geological Society Special Publications, 75, 105–111, doi: 10.1144/GSL.75.105–111.

- Garg, V., Nikam, B., Thakur, P., Aggarwal, S., Gupta, P., & Srivastav, S. (2019). Human-induced land use land cover change and its impact on hydrology. *HydroResearch*, 1, 48-56. DOI: 10.1016/j.hydres.2019.06.001.
- Guerschman, J. P., Paruelo, J. M., Di Bella, C., Giallorenzi, M. C., & Pacin, F. (2003). Land cover classification in the Argentine Pampas using multi-temporal Landsat TM data. *International Journal of Remote Sensing*, 24(17), 3381–3402. <https://doi.org/10.1080/0143116021000021288>
- Hazarika, N., Das, A. K., & Borah, S. B. (2015). Assessing land-use changes driven by river dynamics in chronically flood affected Upper Brahmaputra plains, India, using RS-GIS techniques. *The Egyptian Journal of Remote Sensing and Space Science*, 18(1), 107-118.
- <https://www.sciencedirect.com/science/article/pii/S1110982315000022>
- Horacio, J. (2014). River sinuosity index: geomorphological characterisation. CIREF and Wetlands International European Association, 8p..
- Hu, H., Liu, W., & Cao, M. (2008). Impact of land use and land cover changes on ecosystem services in Menglung, Xishuangbanna, Southwest China. Environmental monitoring and assessment, 146, 147-156. <https://doi.org/10.1007/s10661-007-0067-7>
- Jaquet, S., Schwilch, G., Hartung-Hofmann, F., Adhikari, A., Sudmeier-Rieux, K., Shrestha, G., ... & Kohler, T. (2015). Does outmigration lead to land degradation? Labour shortage and land management in a western Nepal watershed. *Applied geography*, 62, 157-170. <https://www.sciencedirect.com/science/article/pii/S014362281500096X>
- K. C., B., Wang, T., & Gentle, P. (2017). Internal Migration and Land Use and Land Cover Changes in the Middle Mountains of Nepal. *Mountain Research and Development*, 37(4), 446–455. <https://doi.org/10.1659/MRD-JOURNAL-D-17-00027.1>
- Karki, S. (2011). GIS based flood hazard mapping and vulnerability assessment due to climate change: a case study from Kankai watershed, Eastern Nepal. <https://doi.org/10.13140/RG.2.1.4993.2965>
- Kayet, N., Chakrabarty, A., Pathak, K., Sahoo, S., Mandal, S. P., Fatema, S., ... & Das, T. (2019). Spatiotemporal LULC change impacts on groundwater table in Jhargram, West Bengal, India. *Sustainable Water Resources Management*, 5, 1189-1200. <https://doi.org/10.1007/s40899-018-0294-9>

- Kumari, M., Das, A., Sharma, R., & Saikia, S. (2014). Change detection analysis using multi temporal satellite data of Poba reserve forest, Assam and Arunachal Pradesh. *International Journal of Geomatics and Geosciences*, 4(3), 517-525. <https://www.researchgate.net/publication/270280879>
- Lambin, E. F. (1997). Modelling and monitoring land-cover change processes in tropical regions. *Progress in physical geography*, 21(3), 375-393. <https://doi.org/10.1177/030913339702100303>
- Lamichhane, B. R. (2008). Dynamics and driving forces of land use/forest cover change and indicators of climate change in a mountain sub-watershed of Gorkha (Doctoral dissertation, Thesis submitted in partial fulfillment of the award of M Sc NRMRD to Tribhuvan University/Institute of Forestry, Pokhara, Nepal). <https://doi.org/10.13140/RG.2.2.32328.78085>
- Langat, P. K., Kumar, L., & Koech, R. (2019). Monitoring river channel dynamics using remote sensing and GIS techniques. *Geomorphology*, 325, 92-102. <https://www.sciencedirect.com/science/article/pii/S0169555X18304070>
- Lillesand, T., Kiefer, R. W., & Chipman, J. (2015). Remote sensing and image interpretation. John Wiley & Sons.
- Liu, X. H., Skidmore, A. K., & Van Oosten, H. (2002). Integration of classification methods for improvement of land-cover map accuracy. *ISPRS Journal of Photogrammetry and Remote Sensing*, 56(4), 257-268. www.elsevier.com/locate/isprsjprs
- López-Granados, E., Mendoza, M. E., & González, D. I. (2013). Linking geomorphologic knowledge, RS and GIS techniques for analyzing land cover and land use change: a multitemporal study in the Cointzio watershed, Mexico. *Revista Ambiente & Água*, 8, 18-37. https://www.scielo.br/scielo.php?pid=S1980-993X2013000100003&script=sci_arttext
- Manandhar, R., Odeh, I. O., & Ancev, T. (2009). Improving the accuracy of land use and land cover classification of Landsat data using post-classification enhancement. *Remote Sensing*, 1(3), 330-344. <https://doi.org/10.3390/rs1030330>
- Mandal, U. K. (2014). Geo-information based spatio-temporal modeling of urban land use and land cover change in Butwal municipality, Nepal. *The International Archives of Photogrammetry, Remote Sensing and Spatial Information Sciences*, 40(8), 809. <https://doi.org/10.5194/isprsarchives-XL-8-809-2014>

- Mueller, J. E. (1968). An introduction to the hydraulic and topographic sinuosity indexes. *Annals of the association of american geographers*, 58(2), 371-385. <https://doi.org/10.1111/j.1467-8306.1968.tb00650.x>
- Mundia, C. N., & Murayama, Y. (2010). Modeling spatial processes of urban growth in African cities: A case study of Nairobi City. *Urban Geography*, 31(2), 259-272. <https://doi.org/10.2747/0272-3638.31.2.259>
- Neupane, K. (2016). An Assessment of Land Use Land cover Change in Barandabhar Forest Corridor, Chitwan District, Nepal. *Bachelor of Science in Forestry Degree. Tribhuvan University, Kathmandu Forestry College, Kathmandu, Nepal.*
- Niraula, R., Gilani, H., Niraula, R. R., Kumar Pokharel, B., Mueen Qamer, F., & Ghat, D. (2013). Measuring impacts of community forestry program through repeat photography and satellite remote sensing in the Dolakha district of Nepal. *Journal of Environmental Management*, 126, 20–29. <https://doi.org/10.1016/j.jenvman.2013.04.006>
- Núñez, M. N., Ciapessoni, H. H., Rolla, A., Kalnay, E., & Cai, M. (2008). Impact of land use and precipitation changes on surface temperature trends in Argentina. *Journal of Geophysical Research Atmospheres*, 113(6). <https://doi.org/10.1029/2007JD008638>
- Ozturk, D., & Sesli, F. A. (2015). Determination of temporal changes in the sinuosity and braiding characteristics of the Kizilirmak River, Turkey. *Polish Journal of Environmental Studies*, 24(5), 2095–2112. <https://doi.org/10.15244/pjoes/58765>
- Pandey, D., Heyojoo, B. P., & Shahi, H. (2016). Drivers and dynamics of land use land cover in Ambung VDC of Tehrathum district, Nepal. *Banko Janakari*, 26(1), 90-96. <https://www.nepjol.info/index.php/BANKO/article/view/15508>
- Paudel, B., Zhang, Y. li, Li, S. cheng, Liu, L. shan, Wu, X., & Khanal, N. R. (2016). Review of studies on land use and land cover change in Nepal. *Journal of Mountain Science*, 13(4), 643–660. <https://doi.org/10.1007/s11629-015-3604-9>
- Rahman, A., Kumar, S., Fazal, S., & Siddiqui, M. A. (2012). Assessment of Land use/land cover Change in the North-West District of Delhi Using Remote Sensing and GIS Techniques. *Journal of the Indian Society of Remote Sensing*, 40(4), 689–697. <https://doi.org/10.1007/s12524-011-0165-4>

- Rai, R., Zhang, Y., Paudel, B., Kumar Acharya, B., & Basnet, L. (2018). Land Use and Land Cover Dynamics and Assessing the Ecosystem Service Values in the Trans-Boundary Gandaki River Basin, Central Himalayas. *MDPI*, 10, 3052. <https://doi.org/10.3390/su10093052>
- Rawat, J., Biswas, V., Sensing, M. K.-T. E. J. of R., & 2013, U. (2013). Changes in land use/cover using geospatial techniques: A case study of Ramnagar town area, district Nainital, Uttarakhand, India. *The Egyptian Journal of Remote Sensing and Space Science*, 111–117. <https://www.sciencedirect.com/science/article/pii/S1110982313000069>
- Regmi, R. R., Saha, S. K., & Subedi, D. S. (2017). Geospatial analysis of land use land cover change modeling in Phewa Lake watershed of Nepal by using GEOMOD model. *Himalayan Physics*, 65-72. <https://www.nepjol.info/index.php/HP/article/view/18363>
- Reis, S. (2008). Analyzing Land Use/Land Cover Changes Using Remote Sensing and GIS in Rize, North-East Turkey. *Sensors*, 8(10), 6188–6202. <https://doi.org/10.3390/s8106188>
- Ruslan, R. (2003). GIS Application in Evaluating Land Use-Land Cover change and its Impact on Hydrological Regime in Langat River Basin, Malaysia Changing patterns of racial diversity in Peninsular Malaysia 1980-2010 View project. <https://www.researchgate.net/publication/255590921>
- Rwanga, S. J. N.-. (2017). Accuracy assessment of land use/land cover classification using remote sensing and GIS. *Scirp.Org*, 8(4), 611. https://www.scirp.org/html/14-2801413_75926.htm
- Sapkale, J. B., Kadam, Y. U., Jadhav, I. A., & Kamble, S. S. (2016). River in Planform and Variation in Sinuosity Index : A Study of Dhamni River, Kolhapur (Maharashtra), India. *India Article in International Journal of Scientific and Engineering Research*, 7(2). <http://www.ijser.org>
- Schumm, S. A. (1963). Sinuosity of alluvial rivers on the great plains. *Bulletin of the Geological Society of America*, 74(9), 1089–1100. [https://doi.org/10.1130/0016-7606\(1963\)74\[1089:SOAROT\]2.0.CO;2](https://doi.org/10.1130/0016-7606(1963)74[1089:SOAROT]2.0.CO;2)
- Serra, P., Pons, X., & Saurí, D. (2008). Land-cover and land-use change in a Mediterranean landscape: a spatial analysis of driving forces integrating biophysical and human factors. *Applied geography*, 28(3), 189-209.

- Subedee, B. R., Chaudhary, R. P., Shrestha, K. R., & Dorji, T. (2017). Use of Rocket stove for firewood savings and carbon emission reductions by the households involved in Allo (*Girardinia diversifolia*) fiber processing at Khar VDC, Darchula District, Nepal. *International Journal of Latest Engineering and Management Research*, 2, 28-35. <https://doi.org/10.1016/B978-0-12-394847-2.00020-6>
- Sun, Z., Guo, H., Li, X., Huang, Q., & Zhang, D. (2011, May). Effect of LULC change on surface runoff in urbanization area. In *Proceedings of the ASPRS 2011 Annual Conference, Milwaukee, Wisconsin, May* (Vol. 1, No. 5). <https://www.asprs.org/wpcontent/uploads/2010/12/Sun.pdf>
- Tamrakar, N. K., Bajracharya, R., & Shrestha, P. (2011). River dynamics and existing stability condition of the Manahara River, Kathmandu basin, Central Nepal Himalaya. *Bulletin of the Department of Geology*, 14, 1–8. <https://doi.org/10.3126/bdg.v14i0.5430>
- Thakur, B., & Singh, D. Sen. (2018). The Rapti River: Odyssey from Nepal to India (pp. 165–175). https://doi.org/10.1007/978-981-10-2984-4_13
- Tilahun, A., & Teferie, B. (2015). Accuracy Assessment of Land Use Land Cover Classification using Google Earth. *American Journal of Environmental Protection*, 4(4), 193–198. <https://doi.org/10.11648/j.ajep.20150404.14>
- Uddin, K., Shrestha, H. L., Murthy, M. S. R., Bajracharya, B., Shrestha, B., Gilani, H., ... & Dangol, B. (2015). Development of 2010 national land cover database for the Nepal. *Journal of environmental management*, 148, 82-90. <https://www.sciencedirect.com/science/article/pii/S0301479714004009>
- Verheye, W. H. (Ed.). (2009). *Land use, land cover and soil sciences-volume IV: Land use management and case studies*. EOLSS Publications.
- Weber, C., & Puissant, A. (2003). Urbanization pressure and modeling of urban growth: example of the Tunis Metropolitan Area. *Remote sensing of environment*, 86(3), 341-352. <https://www.sciencedirect.com/science/article/pii/S0034425703000774>
- Yang, G., Chao, S., Tsou, J. Y., & Zhang, Y. (2019). Satellite image-based methods of spatiotemporal analysis on sustainable urban land use change and the driving factors: A case study in caofeidian and the suburbs, China. *Sustainability*, 11(10), 2927. <https://doi.org/10.3390/su11102927>
- Yousefi, S., Pourghasemi, H. R., Hooke, J., Navratil, O., & Kidová, A. (2016). Changes in morphometric

meander parameters identified on the Karoon River, Iran, using remote sensing data. *Geomorphology*, 271, 55-64. <https://www.sciencedirect.com/science/article/pii/S0169555X1630647X>

Zubair, O. A., & Ji, W. (2015). Assessing the Impact of Land Cover Classification Methods on the Accuracy of Urban Land Change Prediction. *Canadian Journal of Remote Sensing*, 41(3), 170–190. <https://doi.org/10.1080/07038992.2015.1065706>